

Low-energy excitations in amorphous films of silicon and germanium

Xiao Liu and R. O. Pohl*

Laboratory of Atomic and Solid State Physics, Cornell University, Ithaca, New York 14853-2501

(Received 6 May 1998)

We present measurements of internal friction and shear modulus of amorphous Si (*a*-Si) and amorphous Ge (*a*-Ge) films on double-paddle oscillators at 5500 Hz from 0.5 K up to room temperature. The temperature-independent plateau in internal friction below 10 K, which is common to all amorphous solids, also exists in these films. However, its magnitude is smaller than found for all other amorphous solids studied to date. Furthermore, it depends critically on the deposition methods. For *a*-Si films, it decreases in the sequence of electron-beam evaporation, sputtering, self-ion implantation, and hot-wire chemical-vapor deposition (HWCVD). Annealing can also reduce the internal friction of the amorphous films considerably. Hydrogenated *a*-Si with 1 at.% H prepared by HWCVD leads to an internal friction more than two orders of magnitude smaller than observed for all other amorphous solids. The internal friction increases after the hydrogen is removed by effusion. Our results are compared with earlier measurements on *a*-Si and *a*-Ge films, none of which had the sensitivity achieved here. The variability of the low-energy tunneling states in the *a*-Si and *a*-Ge films may be a consequence of the tetrahedrally bonded covalent continuous random network. The perfection of this network, however, depends critically on the preparation conditions, with hydrogen incorporation playing a particularly important role. [S0163-1829(98)07838-2]

I. INTRODUCTION

In spite of the rapid development of amorphous Si (*a*-Si) and amorphous Ge (*a*-Ge) technology in solar cells, thin-film transistors, flat panel displays, and many other applications, many fundamental questions concerning these tetrahedrally bonded amorphous semiconductors and their possible relation to the electronic and optical properties of these materials still remain unanswered. An example is the low-energy vibrational excitations in these solids, which are the subject of this investigation.

Shortly after the discovery of the anomalous low-temperature properties of amorphous solids which indicate the existence of a broad distribution of low-energy excitations in addition to propagating phonons,¹ it was proposed that these low-energy excitations are caused by tunneling of atoms or groups of atoms between nearly degenerate equilibrium positions.^{2,3} As a consequence, it was argued³ that the tunneling motion is expected to be much less likely to occur in tetrahedrally bonded amorphous solids because of their overconstrained structure which restricts the atomic motion. Thus, it was hoped that by probing the absence of tunneling states in *a*-Si and *a*-Ge a microscopic foundation for the two-level tunneling system (TLS) model would be provided, which had been highly successful in providing a phenomenological description of the thermal and elastic properties of amorphous solids.⁴

However, in spite of much experimental effort, it remained unclear whether or not the low-energy excitations exist in *a*-Si and *a*-Ge. This uncertainty is mainly due to the fact that *a*-Si and *a*-Ge can only be prepared as thin films which are poorly suited for the standard techniques used to detect those states, i.e., thermal conductivity, specific heat, and acoustic waves. For example, the thermal conductivity of *a*-Ge films was found to be dominated by Rayleigh and boundary scattering,^{5,6} which made it difficult to identify the

expected T^2 temperature dependence below 1 K. Specific-heat measurements on *a*-Ge (Refs. 7–9) and *a*-Si (Refs. 10,11) films could not resolve the typical linear temperature dependence, and resulted only in upper limits of the density of tunneling states. These were determined to be somewhat smaller than those observed in other amorphous solids, e.g., by a factor of 5 smaller than in amorphous SiO₂ (*a*-SiO₂) at most. The technique of surface acoustic waves was applied to search for the logarithmic temperature dependence of the relative variation in sound velocity at low temperatures.^{12–15} However, the results were conflicting, possibly because of the limited sensitivity of the technique and influence of accidentally incorporated impurities during sample preparations and heat treatments.

Another problem may arise from the fact that thin films prepared by condensation from the vapor phase are further away from the equilibrium state than amorphous solids produced by quenching from the melt. Therefore their physical properties might depend on the preparation methods, variable conditions within each method, heat treatments,¹⁶ and incorporation of hydrogen.¹⁷ The influence of these additional parameters on the low-energy excitations in *a*-Si and *a*-Ge films may have been important in earlier experiments and requires a more systematic study.

The objective of the study reported here is to use the double-paddle oscillator technique to investigate the low-energy excitations in *a*-Si and *a*-Ge films. This technique was developed specifically to probe the low-energy excitations in thin films.¹⁸ It has been found that the background damping of the torsional oscillation of double-paddle oscillators is extremely low (internal friction $Q^{-1} \sim 10^{-8}$) so that the low-temperature internal friction of thin films deposited onto them can be studied with great sensitivity. This technique has been used successfully to detect energy dissipation caused by films of *a*-SiO₂ as thin as 7.5 Å.¹⁹ Using the same technique, we are now able to show unambiguously the ex-

TABLE I. The parameters of the TLS model, $\bar{P}\gamma^2$ and C (see text for explanation), obtained from earlier measurements are compared with those determined in this work. For simplicity, we use the transverse sound velocity in all cases. This introduces typically about 20% error in converting \bar{P} obtained in specific-heat measurements to C . The relationship between sound velocities of transverse and Rayleigh waves is unknown. However, as has been frequently done in earlier work (Ref.13), we assume $v_R \approx v_t$ in this work as well. We assume the coupling energy γ for all a -Si and a -Ge films listed here to be the same as that determined by Duquesne and Bellessa for a -Ge (Ref. 13). Parameters in brackets are not originally given in the references cited in column 2. They are introduced or calculated here to complete the comparison. The symbols α , $\Delta v/v_0$, and C_p in column 2 have the meaning of acoustic attenuation, variation of sound velocity, and specific heat, respectively. For the sake of clarity, the results of earlier work on the a -Si:H films are not included in this table.

Samples	References	ρ (g/cm ³)	v (10 ⁵ cm/s)	Previous work				This work ^a	
				\bar{P} (10 ³¹ /erg cm ³)	γ (eV)	$\bar{P}\gamma^2$ (10 ⁷ erg/cm ³)	C (10 ⁻⁵)	$\bar{P}\gamma^2$ (10 ⁷ erg/cm ³)	C (10 ⁻⁵)
e -beam a -Ge	C_p (Ref. 9)	(4.2)	(1.92)	<1.4	(0.36)	(<0.53)	(<3.4)	0.7	4.5
e -beam a -Si	C_p (Ref. 11)	(2.1)	(3.85)	<5.4	(0.36)	(<1.8)	(<5.8)	3.0	8.3
Sputtered a -Si	α (Ref. 12)	(2.1)	(3.85)	(7.8)	(0.36)	2.6	8.2	1.2	3.8
Sputtered a -Si	$\Delta v/v_0$ (Ref. 12)	(2.1)	(3.85)	(4.5)	(0.36)	<1.5	<4.8	1.2	3.8
Sputtered a -Ge	α (Ref. 14)	(4.2)	(1.92)	(2.1)	(0.36)	0.71	4.1	0.7	4.5
Sputtered a -Ge	α (Ref. 13)	4.7	3.2	(4.0)	0.36	1.35	2.8	0.7	4.5
Sputtered a -Ge	$\Delta v/v_0$ (Ref. 13)	4.7	3.2	(4.0)	0.36	1.35	2.8	0.7	4.5
Sputtered a -Si	α (Ref. 15)	2.0	4.0	(3.0)	(0.36)	1.0	3.1	1.2	3.8
Sputtered a -Si	$\Delta v/v_0$ (Ref. 15)	2.0	4.0	(1.1)	(0.36)	3.5	11.0	1.2	3.8
Bulk a -SiO ₂	(Ref. 22)	2.2	3.8	8	0.65	9.2	29.0		

^aDetermined from internal friction plateau and G_{film} as given in Sec. IV.

istence of the low-energy excitations in both a -Si and a -Ge films, and will report here that they resemble those of all amorphous solids. Their concentration, however, as measured through the magnitude of the temperature-independent plateau of the low-temperature internal friction, Q_0^{-1} , can vary over two orders of magnitude and depends critically on film preparation and heat treatment. Among the a -Si and a -Ge films studied in this work, the highest internal friction is found in e -beam a -Si films, but even its Q_0^{-1} is smaller than that of any known amorphous solid studied to date. The smallest Q_0^{-1} has been found for certain hydrogenated a -Si (a -Si:H) films as reported recently.²⁰ The variability of the low-energy excitations in these tetrahedrally bonded amorphous thin films is in contrast to the universality of the low-energy tunneling states in all other amorphous solids, in which values of Q_0^{-1} range between 1.5×10^{-3} and 1.5×10^{-4} (Ref. 21)—the so-called “glassy range.” Possible reasons for this different behavior in a -Si and a -Ge will be discussed, and may shed new light on the microscopic origin of the intriguing low-energy excitations.

The outline of the paper is as follows. In Sec. II, a review of the earlier investigations will be given including their analyses within the TLS model. In Sec. III, the experimental method employed here will be presented. In Sec. IV, film preparation and characterization will be described, and also some of the film properties, like mass density and shear modulus, which are needed for the evaluation of our measurements, will be summarized. Sections V, VI, and VII contain the experimental results, discussion, and conclusion.

II. REVIEW OF EARLIER WORK WITHIN THE TLS MODEL

According to the TLS model, a wide distribution of the asymmetry ϵ and of the tunneling parameter λ which de-

scribes the overlap of the wave functions of double-well potentials leads to a constant spectral density of tunneling states $P(\epsilon, \lambda) = \bar{P}$. This in turn yields the linear specific heat commonly observed in amorphous solids:

$$C_p = \frac{\pi^2}{12} k_B^2 \bar{P} T \ln \frac{4t}{\tau_{\min}}, \quad (1)$$

where k_B is Boltzmann's constant, t the measuring time, and τ_{\min} the minimum relaxation time of the tunneling states. For a typical measuring time (1 to 10 s) at low temperatures ($T < 1$ K), one finds²² $\ln(4t/\tau_{\min}) \approx 20$.

In measurements of the low-temperature specific heat of sputtered a -Ge (Ref. 7) and a -Si (Ref. 10) films performed above 1 K, a softening of the lattice has been observed. This softening, a prelude for possible tunneling states at lower temperature, was confirmed by inelastic neutron scattering measurements.²³ The specific-heat measurements of both e -beam a -Ge (Refs. 8,9) and a -Si (Ref. 11) films performed below 1 K was found to be dominated by magnetic contributions arising from exchange-coupled clustering of dangling bonds. After suppressing the magnetic contribution by applying a 6 T magnetic field, an upper limit for a magnetic field-independent linear term was given. It translated to an upper limit for \bar{P} of 1.4×10^{31} and 5.4×10^{31} erg⁻¹ cm⁻³ for e -beam a -Ge and a -Si films, respectively, somewhat smaller than that of a -SiO₂;²² see Table I for comparison. However, since the measurements were done almost within the detection limit of the technique, it could be safely concluded only that if there were tunneling states, their density ought to be smaller than in a -SiO₂.

Much work was done using surface acoustic waves, the so-called Rayleigh waves. Such waves propagate in the thin film, and sometimes also extend into the substrate. Tunneling states can be probed by the logarithmic rise of the relative

variation of sound velocity v with increasing temperature due to the resonant scattering of phonons by those states at low temperatures:

$$\left(\frac{\Delta v}{v_0}\right) = \frac{v - v_0}{v_0} = C \cdot \ln \frac{T}{T_0}, \quad (2)$$

where v_0 is the sound velocity at an arbitrary reference temperature T_0 , and C is the tunneling strength given by

$$C = C_{l,t} = \frac{\bar{P} \gamma_{l,t}^2}{\rho v_{l,t}^2}, \quad (3)$$

where $\gamma_{l,t}$ is the coupling energy of the phonons to the tunneling entities, and the subscripts denote the coupling energy of transverse (t) and longitudinal (l) phonons. Since C has been found to be insensitive to the modes of the sound wave, we omit those subscripts here and in the following.

The quantity C appears not only in the expression of the relative variation of sound velocity [Eq. (2)], but also in the thermal conductivity and the internal friction at low temperatures. The internal friction plateau below 10 K is a direct measure of C with

$$Q_0^{-1} = \frac{\pi}{2} C. \quad (4)$$

Although the individual quantities in the expression for C may vary by more than two orders of magnitude, the quantity C is found to have a value between 10^{-4} and 10^{-3} for all amorphous solids studied so far.²⁴ This is the universality of the anomalous low-temperature properties of amorphous solids referred to above. Therefore, internal friction measurements at low temperatures, as will be presented in this paper, offer a simple way to detect low-energy excitations without mathematical complications.

Ultrasonic attenuation, α , which can also be probed by surface acoustic waves, relates directly to the internal friction by $Q^{-1} = (v/\omega)\alpha$.²⁵ However, one has to keep in mind that the evaluation of the Rayleigh wave attenuation is complicated due to the spatial inhomogeneity of the deformation field,¹³ which causes difficulties in determining the coupling energy γ_R and sound velocity v_R of Rayleigh waves.

Sputtered a -Si films were investigated by v. Haumerer *et al.*¹² using surface acoustic waves. The relative variation of sound velocity did not show a logarithmic temperature dependence as predicted in Eq. (2). Instead only an upper limit of $\bar{P} \gamma^2$ was given, which was smaller than that of a -SiO₂; see Table I for comparison. This failure to probe the tunneling states was attributed to the film thicknesses which were smaller than the penetration depths, so that a large proportion of the sound wave travelled in the substrate, masking the effect of the tunneling states as suggested by Duquesne and Bellesa.¹³ Although the authors¹² did observe an attenuation shoulder at about 10 K, typical of tunneling states at 300 MHz, they suspected it to be caused by residual oxygen impurities accidentally incorporated during deposition. In a similar study on sputtered a -Ge films by Bhatia *et al.*,¹⁴ a similar conclusion was drawn.

Subsequent measurements of sputtered a -Ge films by Duquesne and Bellesa¹³ identified the logarithmic temperature

dependence of $\Delta v/v_0$ using much thicker films so that the Rayleigh waves propagated only in the film. In addition, the authors demonstrated that the logarithmic temperature dependence could also vanish when the frequency was reduced so that the Rayleigh waves extended into the substrate. These authors were able to present a consistent description of the relative variation of sound velocity and of the acoustic absorption using a single set of parameters on the basis of the TLS model.¹³ These parameters are summarized in Table I. Annealing at 350 °C for 5 h did not cause a reduction of the tunneling states, but a 20% increase of C . The authors considered this as conclusive evidence of the atomic tunneling states in these films, since it is known that heat treatment hardly affects the tunneling states in bulk amorphous solids.²⁶ However, it has also been suggested¹⁴ that oxygen impurities might be extremely effective in forming tunneling states in a -Ge films. We consider this to be a likely explanation because of the low deposition rate and the relatively poor vacuum used in these experiments during deposition and annealing. As a demonstration of the high sticking probability of oxygen onto vaporized Si atoms, we e -beam evaporated a -Si under a vacuum of $\sim 10^{-6}$ torr with a deposition rate of 10 Å/s. The oxygen content was found to be 20 at. % as checked by Rutherford backscattering spectrometry (RBS). As will be demonstrated in this work, a significant reduction in the density of the tunneling states in thin films of very pure a -Si and a -Ge may indeed be possible upon thermal annealing.

Measurements on sputtered a -Si films by Tokumoto *et al.*¹⁵ also revealed the existence of tunneling states through a logarithmic temperature dependence of $\Delta v/v_0$, consistent with the results by Duquesne and Bellesa on sputtered a -Ge films.¹³ Again, see Table I for the parameters derived by Tokumoto *et al.* While the authors attributed the shoulder of the acoustic absorption at 10 K to oxygen impurities, they concluded that the effect observed in the variation of the sound velocity was not affected by oxygen although a 50% increase of $\bar{P} \gamma^2$ was observed after exposure to air for 6 months.¹⁵ It has been found that exposure of a -Si films to air will not change the oxygen content as much as depositing or annealing in poor vacuum.¹⁶ We suggest that more careful surface acoustic wave measurements are required to clarify the influence of deposition conditions and the effect of annealing in a -Si and a -Ge films.

For the various a -Si and a -Ge films studied, the coupling energy γ was determined only for sputtered a -Ge films by Duquesne and Bellesa.¹³ Assuming the same value of γ for all other a -Si and a -Ge films, one can make a rough comparison between quantities determined in specific heat measurements and in acoustic or elastic measurements. This is done in Table I. As can be seen, the agreement of the values or the upper limits of $\bar{P} \gamma^2$ and C determined by specific heat and by surface acoustic waves is in fact reasonably good.

The limited suitability of the dielectric and thermal conductivity experiments for detecting tunneling states in a -Si and a -Ge films has been thoroughly discussed by Duquesne and Bellesa.¹³ Therefore, we will not review those measurements here.

There have been some experimental efforts to determine the existence of tunneling states in a -Si:H and a -Ge:H films

as well. Specific-heat measurements by v. Löhneysen of an a -Si:H film with 35 at. % H prepared by plasma-enhanced chemical-vapor deposition (PECVD) onto a crystalline Si substrate held at room temperature²⁷ indicated contributions from both tunneling states and magnetic excitations which disappeared after annealing at 210 °C. A combined study of specific heat and thermal conductivity of PECVD a -Si:H films with 17 at. % H deposited at 120–180 °C by Graebner *et al.*²⁸ showed evidence for a spectral density of tunneling states $\bar{P}=9\times 10^{31}$ erg⁻¹ cm⁻³, similar to that in a -SiO₂, which was attributed to both intrinsic tunneling states as in H-free a -Si films and H related ones involving the motion of hydrogen atoms. In contrast to the specific-heat study by v. Löhneysen,²⁷ no sign of a magnetic contribution could be inferred, which might be due to the elevated deposition temperature. We have to point out that thermal conductivity measurements performed on the same sample also suffered from the complications discussed in Ref. 13, where four independent parameters were used to fit three phonon scattering processes.²⁸

Observation of tunneling states in PECVD a -Si:H films was also reported in the logarithmic temperature dependence of $\Delta v/v_0$ using surface acoustic waves,¹⁷ where the $\bar{P}\gamma^2$ was found to increase from 6×10^7 erg/cm³ for a -Si:H containing 14 at. % H, to 4.2×10^8 erg/cm³ with 27 at. % H. The value of $\bar{P}\gamma^2$ for a -SiO₂ (see Table I) lies between those two values. A similar increase of the acoustic absorption with increasing H content was observed as well.¹⁷ However, applying the same surface acoustic wave technique, tunneling states were not observed in sputtered a -Si:H (Ref. 29) or a -Ge:H films (Ref. 30) with H concentrations up to 15 and 25 at. %, respectively. This again might be due to the insensitivity caused by the relatively thin-film thicknesses used in those experiments. However, a nonmonotonic dependence of the acoustic absorption on the H content was observed in sputtered a -Si:H films (but not in sputtered a -Ge:H) with a maximum absorption at 1.5 at. % H.²⁹

In view of these earlier investigations, there is only limited information on the tunneling states in a -Ge and a -Si, and no clear picture as to the effect of hydrogen. Moreover, most of the earlier results are limited by the sensitivity of the techniques used.

III. EXPERIMENTAL METHOD

The fabrication and use of double-paddle oscillators have been described in Ref. 18 and references therein. Here we only summarize some points directly related to this work.

The double-paddle oscillators shown in Fig. 1 are fabricated from superpure, undoped, float-zone silicon wafers ($\langle 100 \rangle$ oriented, 300 ± 5 μ m thick) with room-temperature electrical resistivities greater than 10 k Ω cm. The head and wings are connected by a narrow neck about 1 mm wide. The wings in turn are connected to the foot by a leg which is longer and narrower than the neck. The foot is attached with Stycast 2850 FT epoxy to an Invar block, the thermal expansion of which closely matches that of crystalline silicon. A metal film (30 Å Cr + 500 Å Au) is then evaporated on the back side of the oscillator, without coating the neck and head. This film makes electrical contact to the Invar block

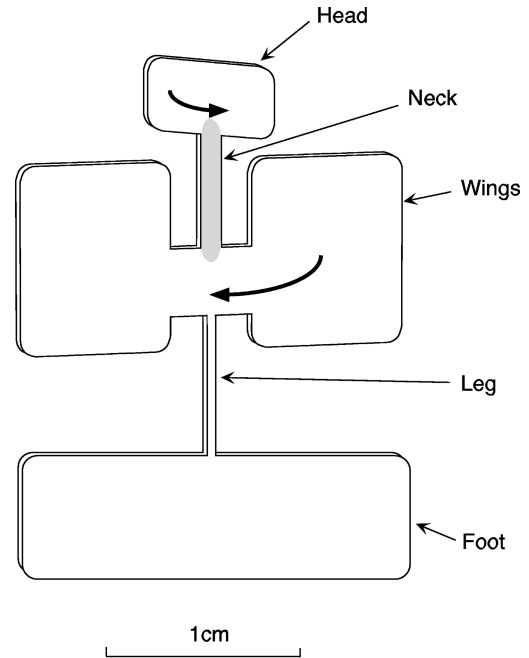


FIG. 1. The double-paddle oscillator: the arrows illustrate the oscillation in the antisymmetric mode. Thin films of interest are deposited or ion-implanted on the shaded area of the neck.

which is electrically grounded to the cryostat, so that the oscillator can be excited capacitively into its resonant modes. The driving and detection circuit is kept in a phase-locked loop, so that the resonant frequency can be measured accurately (1 part in 10^8). The internal friction is measured from the free amplitude decay after the driving force is turned off. The antisymmetric mode, with a resonant frequency of ~ 5500 Hz, has an extremely small internal friction ($Q^{-1} \sim 10^{-8}$) at low temperatures. In this mode the head and the wings vibrate out of phase, twisting the neck as illustrated in Fig. 1 by the arrows. The small rotational inertia of the head relative to that of the wings minimizes the twisting of the leg. This greatly reduces the clamping loss. In addition, since the metal film does not cover the neck, the energy dissipation of the metal film to the antisymmetric mode can be minimized.³¹ This special design ensures an exceptionally small damping of the oscillator, so that very thin films or films with very little internal friction can be studied when they are deposited onto the neck.^{19,20}

The symmetric mode, in which the leg is twisted by the in-phase oscillation of the head and wings with a resonant frequency of ~ 410 Hz, is also used. Due to the clamping of the foot, the damping of this mode is more than one order of magnitude higher than that of the antisymmetric mode, making it less sensitive for the internal friction study of thin films. However, by not coating the leg with the thin film of interest, the resonant frequency shift of the symmetric mode before and after the film is deposited on the neck and wings is solely determined by the mass increase while the resonant frequency shift of the antisymmetric mode is determined by both the mass increase and change in shear modulus of the paddle oscillator. This provides a way to determine the mass and the shear modulus of the film, as was detailed in Ref. 18.

Before mounting the paddle oscillator, it is cleaned by dipping it in 25% HF followed by acetone, isopropanol, and

deionized water rinses, and blown dry. The HF removes the 800 Å thick amorphous Si₃N₄ layer used as an etch mask during the KOH etching. After this cleaning, the surface of the substrate is considered semiconducting grade clean, and ready for thin-film deposition or implantation (see Sec. IV).

The internal friction is measured in an evacuated ³He cryostat in the temperature range from 0.5 K to room temperature with a sample chamber pressure always smaller than 2×10^{-7} torr. The sample temperature is determined by a calibrated germanium thermometer from 0.5 to 30 K, and a calibrated Pt thermometer from 30 K up to room temperature. Before each data point is taken, the temperature is stabilized until there is no detectable change in resonant frequency of the oscillator. Because of the good vibration isolation, the background internal friction of a bare paddle can be reproduced within 10% from paddle to paddle, and within 1% for the same paddle in separate runs. No strain amplitude dependence was observed for strain amplitude up to 5×10^{-5} .

Deposition of a thin film (layer) onto the double-paddle oscillator will change the internal friction of the paddle (Q_{paddle}^{-1}). From the increase above the background (Q_{bare}^{-1}), the internal friction of the film *itself* (Q_{film}^{-1}) can be obtained through¹⁸

$$Q_{\text{film}}^{-1} = \frac{G_{\text{sub}} t_{\text{sub}}}{3 G_{\text{film}} t_{\text{film}}} (Q_{\text{paddle}}^{-1} - Q_{\text{bare}}^{-1}), \quad (5)$$

where G and t refer to the shear moduli and thicknesses of the paddle (substrate) and the film (layer), respectively. Since the torsional motion of the neck is along the $\langle 110 \rangle$ orientation, its shear modulus can be calculated from the known elastic constants of Si (Ref. 32) as $G_{\text{sub}} = 6.2 \times 10^{11}$ dyn/cm². As mentioned above, the absolute value of the shear modulus of a thin film can be determined from the resonant frequency shifts of the symmetric and antisymmetric modes before and after the film has been deposited (or ion-implanted).¹⁸ However, this can be done accurately only when the film is deposited *in situ*³³ because the resonant frequency is also slightly sensitive to the mounting. In the present work we therefore calculate G_{film} via

$$G_{\text{film}} = \rho v_t^2, \quad (6)$$

where ρ and v_t are the mass density and the transverse sound velocity of the thin film respectively, inferred from literature. In some cases, it was possible to compare the G_{film} values using both methods (see Sec. IV for details).

The relative variation of the sound velocity of a thin film as the temperature is changed can be measured as follows. If $(\Delta f/f_0)_{\text{sub}}$ is the relative variation of the resonant frequency of the bare oscillator with temperature, with f_0 being the frequency at some reference temperature T_0 ; and if $(\Delta f/f_0)$ is the relative variation of the resonant frequency of the oscillator, also at T_0 , after the deposition of a thin film, the relative variation of the sound velocity of the thin film is given by

$$\left(\frac{\Delta v}{v_0} \right)_{\text{film}} = \frac{G_{\text{sub}} t_{\text{sub}}}{3 G_{\text{film}} t_{\text{film}}} \left[\left(\frac{\Delta f}{f_0} \right) - \left(\frac{\Delta f}{f_0} \right)_{\text{sub}} \right]. \quad (7)$$

For our high-purity silicon oscillators operating at 5500 Hz, there is no observable temperature variation of $(\Delta f/f_0)_{\text{sub}}$ below 1 K for torsional oscillation along the $\langle 110 \rangle$ orientation. $(\Delta f/f_0)_{\text{sub}}$ decreases gradually with increasing temperature above 1 K as the lattice softens due to anharmonicity. Similar behavior has been found in crystalline germanium in the same $\langle 110 \rangle$ orientation in ultrasonic measurement.³⁴

IV. FILM PREPARATION AND CHARACTERIZATION

The e -beam evaporation was done in a high vacuum chamber under a pressure of 2×10^{-7} torr during deposition. The silicon source was the same material as that from which the paddle oscillator was made, while the germanium source was commercially 99.999% pure. They were evaporated from a vitreous coated carbon crucible at normal incidence at a deposition rate of 25 Å/s, while the paddle oscillator was kept below 100 °C by water cooling. The oxygen content in the film was found to be below the detection limit of RBS (1 at. %). In order to check for possible effects of damping due to the interface, three e -beam a -Si films of different thicknesses (43, 500, and 1700 nm) were evaporated separately under identical conditions.

For e -beam a -Si and a -Ge films, the sound velocities used to evaluate our data are 76.8% and 81.6% of the corresponding directionally averaged ones in their crystalline counterparts, respectively, as determined by Cox-Smith *et al.*,³⁵ who found no substrate temperature dependence up to 235 °C during deposition. The mass densities of the a -Si and a -Ge films are uncertain since e -beam films are porous, and their microstructure and mass density depends on the conditions of film preparation and on the thermal history of the films. Following Williamson *et al.*,³⁶ we assume a mass density deficit of 10% relative to the crystalline phase for both e -beam a -Si and a -Ge films and also for both sputtered a -Si and a -Ge films. Applying Eq. (6), we obtain $G_{\text{film}} = 3.63 \times 10^{11}$ dyn/cm² for the e -beam a -Si films and $G_{\text{film}} = 2.90 \times 10^{11}$ dyn/cm² for the e -beam a -Ge films. Adding the fact that no measurable mass density change (<5%) of the films was found by measuring the film thickness with stylus profilometry for e -beam a -Si and a -Ge films after annealing at 350 °C for 5 h, we use the same G_{film} for both as-evaporated and annealed films. As an additional check for our estimation, we determined ρ_{film} and G_{film} of an e -beam a -Si film from the resonant frequency shifts of both antisymmetric and symmetric modes before and after the film had been evaporated without taking the paddle oscillator from its mounting. They were in good agreement with those determined via Eq. (6).

The sputtering was done in a magnetron sputter system. Commercial 99.999% pure targets were used for both silicon and germanium. The argon partial pressure was 4×10^{-3} torr with background pressure of 4×10^{-7} torr, and the substrate was kept at room temperature. Sputtering will incorporate impurities (e.g., Ar) typically a few atomic percent in the thin film, and the films are less stressed than the ones prepared by e -beam evaporation.³⁷ Here we use a shear modulus $G_{\text{film}} = 3.10 \times 10^{11}$ dyn/cm² for sputtered a -Si films and $G_{\text{film}} = 1.60 \times 10^{11}$ dyn/cm² for sputtered a -Ge films, based on sound velocity measurements of Rayleigh³⁸ and

Young's waves.³⁹ The film thickness was found to be unchanged by stylus profilometry after annealing, indicating no measurable mass density increase. Although a 5–10% increase of sound velocity of sputtered *a*-Si films after a 500 °C anneal was mentioned in Ref. 39, this will only change Q_{film}^{-1} by 10–20%, much smaller than the change observed here (see below). Therefore, just as for *e*-beam films, we will ignore the effect of annealing on the shear modulus.

Amorphization of crystalline Si (*c*-Si) induced by self-ion implantation provides a different morphology of *a*-Si. The oscillator was implanted at room temperature using a Varian/Extrion 200-1000 implanter. We used $^{28}\text{Si}^+$ ions to implant one side of the oscillator under an angle of 7° off the axis to avoid channeling. Three energies, 50, 120, and 180 KeV, were used to achieve uniform amorphization, each at a dose of $7 \times 10^{15} \text{ cm}^{-2}$. The average power generated by accelerating the ions was kept below 45 mW/cm² to avoid *in situ* annealing. This resulted in an amorphized silicon layer 330 nm thick, as determined by cross-sectional transmission electron microscopy,⁴⁰ by RBS channeling, and also by a Monte Carlo simulation (TRIM code), all of which agreed very well. In contrast to physical-vapor deposition (PVD) as described above, the structure is dense and no nanovoids can be detected by small-angle x-ray diffraction³⁶ for silicon layers properly amorphized by ion implantation. The mass density of the resulting amorphous structure is only 1.7% smaller than that of *c*-Si.³⁶ Incorporation of impurities should also be much less likely. Since the sound velocity is about 90% of that in *c*-Si,^{38,41} we used $G_{\text{film}} = 5.54 \times 10^{11} \text{ dyn/cm}^2$ for both as-implanted and annealed layers.

For use as a semiconductor, the dangling bonds in *a*-Si films have to be passivated by hydrogen.⁴² Recently, the use of low-pressure hot-wire-assisted chemical-vapor deposition (HWCVD) to improve *a*-Si:H (Refs. 43,44) has received increased attention. Through appropriate choice of conditions, it is possible to produce device quality *a*-Si:H over a wide range of hydrogen concentrations. The HWCVD films are superior both structurally and electronically to the PECVD films for small hydrogen contents (≤ 10 at. %). In particular, HWCVD *a*-Si:H containing as little as 0.07 at. % H exhibits device-quality electronic properties.⁴⁴ This concentration is just sufficient to passivate the dangling bonds, indicating that excess H is not necessary and may indeed be detrimental. In *a*-Si:H, hydrogen is not uniformly distributed throughout the amorphous lattice but rather has its own microstructure. More than 99% of the hydrogen is either bonded as silicon monohydride or dihydride in device quality *a*-Si:H.⁴⁵ In HWCVD *a*-Si:H with 2 at. % H, over 90% of the hydrogen has been observed to form clusters in less than 10% of the total volume.⁴⁶ Isolated hydrogen is distributed over about 20–30% of the total volume,⁴⁶ leaving a major fraction of the volume without hydrogen at all. The structural properties of the HWCVD material with small hydrogen concentrations are also remarkable. Nanovoids cannot be detected by any technique, and x-ray-diffraction measurements⁴⁷ show this material to have a 20% narrower first diffraction peak than PECVD *a*-Si:H, indicating increased medium range order.⁴⁸

HWCVD *a*-Si:H films were grown at the National Renewable Energy Laboratory in a high vacuum single chamber reactor. The base pressure prior to admitting the SiH₄

was about 4×10^{-7} torr. Internal friction results of three HWCVD *a*-Si:H films are presented in this work. Two of them (Nos. HW133 and H71) were of the best device quality, deposited at a rate of 8 Å/s onto the necks of the oscillators held at 380 °C, which led to an incorporation of about 1 at. % H. The third one (No. THD217) was deposited at a rate of 33 Å/s onto the neck of an oscillator held at 300 °C, which resulted in 4 at. % H. The H contents were determined by measurements of the IR absorption strength of the Si-H wagging mode at 630 cm⁻¹ (Ref. 49) on companion samples. Internal friction was measured again for sample H71 and THD217 after the hydrogen was driven out by annealing at 500 °C and 3×10^{-7} torr for 24 h in a quartz tube. The temperature was ramped up at 1 °C/min and down at 0.5 °C/min to avoid both explosive evolution of hydrogen during heating and quenched-in metastable defects during cooling. Since there exist no sound velocity measurements on HWCVD *a*-Si:H films to date, we assumed its shear modulus to be equal to that of silicon layers amorphized by ion-implantation because of their similarly dense structure.⁵⁰

Selected films, especially the HWCVD *a*-Si:H films, were checked for amorphicity by small-angle x-ray diffraction, Raman scattering, electron diffraction, and high-resolution cross-sectional transmission electron microscopy (see Fig. 2 in Ref. 20). They all showed the typical features of amorphous solids with no sign of any inclusion of crystalline phase. Film thicknesses were measured by stylus profilometry, except for the silicon layer amorphized by ion implantation which was described above.

V. EXPERIMENTAL RESULTS

A. Internal friction of *a*-Si films

Figure 2(a) shows the internal friction of paddles carrying 500 nm thick *e*-beam amorphous films, as-evaporated and after annealing at 350 °C for 5 h. The solid line is the background internal friction of a paddle without film. Also shown is the internal friction of a paddle carrying a 400 nm molecular-beam epitaxial (MBE) silicon layer grown at Texas Instruments. This film has no observable effect on the internal friction. Since a high-quality MBE layer is a simple extension of the crystalline silicon substrate, this absence of an effect is to be expected. In contrast, a 500 nm *e*-beam *a*-Si film increases Q_{paddle}^{-1} by more than one order of magnitude. Annealing at 350 °C leads to a reduction of Q_{paddle}^{-1} , although the film remains amorphous.⁵¹ The corresponding internal friction of the *e*-beam *a*-Si films, Q_{film}^{-1} , calculated from these measurements after Eq. (5), is shown in Fig. 2(b). Both the as-evaporated and the annealed films show the characteristic plateau of amorphous solids below 10 K, indicating the existence of a broad distribution of the low-energy excitations with constant spectral density of states \bar{P} . For comparison, the internal friction of bulk *a*-SiO₂, measured at 4500 Hz on a double-paddle oscillator made out of bulk Suprasil-W,⁵² is shown in Fig. 2(b) as a solid line, representing the internal friction of typical amorphous solids. The internal friction of thin *a*-SiO₂ films measured with the same double-paddle oscillator technique was found in good agreement with that of the bulk shown here.¹⁹ For the as-evaporated *a*-Si film, its internal friction plateau value is already slightly

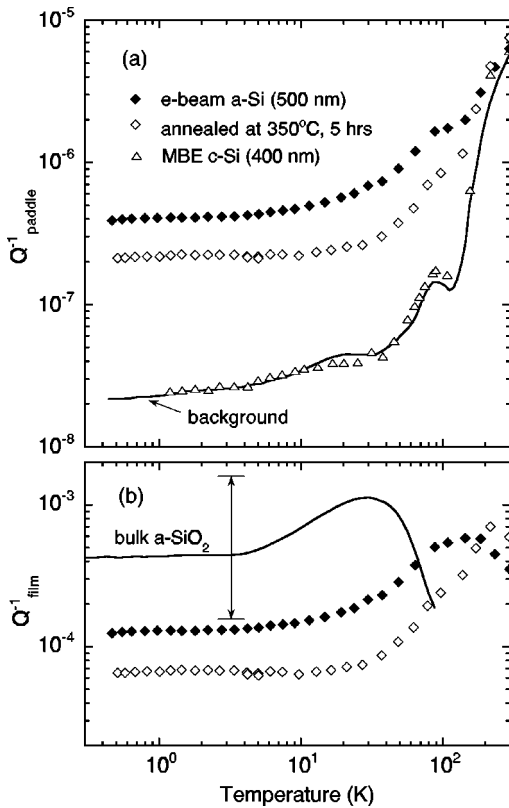


FIG. 2. (a) The internal friction of paddle oscillators carrying vacuum deposited *e*-beam *a*-Si films: as evaporated and annealed at 350 °C for 5 h, and a molecular-beam epitaxial Si layer. The background internal friction of a bare paddle oscillator is shown as a solid line. (b) The internal friction of the same *e*-beam *a*-Si films. Symbols are the same as in (a). The solid line is the internal friction of bulk *a*-SiO₂ (Suprasil W) etched in the same shape as the crystalline silicon paddle oscillator, with resonant frequency of 4500 Hz (Ref. 52). The double arrow demonstrates the “glassy range” explained in text.

below the lower limit of the “glassy range,” as indicated by the double arrow. After annealing, the plateau is reduced by a factor of 2. Since the sound velocity is not expected to change considerably,³⁵ we attribute it to a reduction of the defect states as will be detailed in Sec. VI.

Another feature shown in Fig. 2(b) is a broad relaxation peak centered at about 120 K for the as-evaporated, and at about 200 K for the annealed films. A similar but more pronounced peak has been observed at 270 K in acoustic absorption of as-sputtered *a*-Si films measured at 300 MHz which shifted to 450 K after annealing at 600 K.^{12,29} It has been attributed to thermally activated relaxation of twofold-coordinated Si atoms in the nonideal network of *a*-Si. However, the reason why the peak shifts to higher temperature after annealing is not fully understood.²⁹ Assuming the same mechanism for the peak in our *e*-beam films, we obtain an activation energy of 200 meV for the as-evaporated film from its shift in temperature with frequency, in reasonable agreement to a parametric fit given in Ref. 29.

In order to check for the possible influence of interface related effects on the internal friction, e.g., film adhesion, disorder at the interface, and contamination at the free surface, we measured the internal friction of three paddles carrying *e*-beam *a*-Si films with thicknesses ranging from 43 to

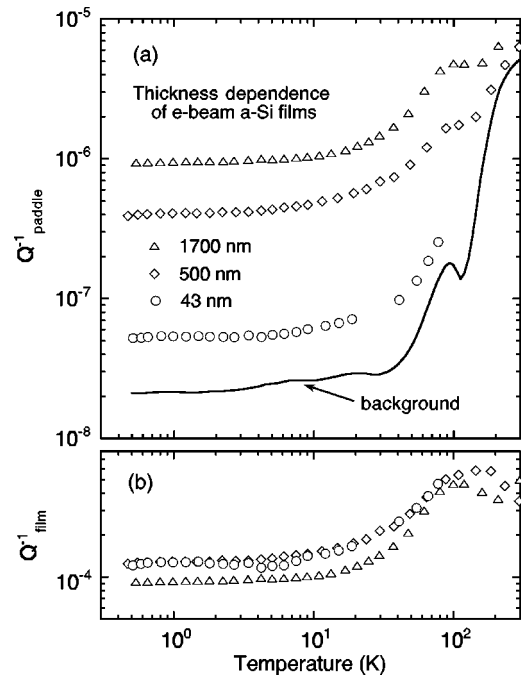


FIG. 3. (a) The internal friction of paddle oscillators carrying *e*-beam *a*-Si films of different thicknesses indicated. The background internal friction of a bare paddle oscillator is shown as a solid line. (b) The internal friction of the same *e*-beam *a*-Si films.

1700 nm. Q_{paddle}^{-1} is shown in Fig. 3(a), while Q_{film}^{-1} is plotted in Fig. 3(b), which agree within 20% for the three different thicknesses. Therefore, no film thickness dependence can be inferred, and we conclude that the Q_{film}^{-1} represents the damping within the films, with no measurable interface effects.

Figure 4 shows the internal friction of a 550 nm thick as-sputtered *a*-Si film and of a companion film which was annealed at 350 °C for 5 h. The internal friction of the as-sputtered *a*-Si film is smaller by a factor of 2.2 than that of the as-evaporated *e*-beam *a*-Si film [see Fig. 2(b)], and lies clearly outside the “glassy range” as shown by the double arrow in Fig. 4. The difference in Q_0^{-1} for *e*-beam and sputtered *a*-Si films demonstrates the influence of the preparation methods on the low-energy excitations in *a*-Si films, in contrast to the fact that no difference in Q_0^{-1} was found in

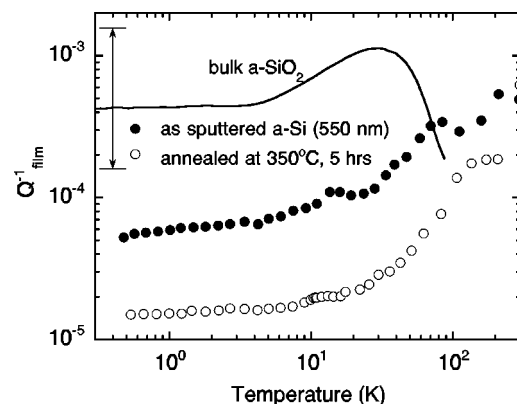


FIG. 4. The internal friction of sputtered *a*-Si films: as sputtered and annealed at 350 °C for 5 h. The solid line and double arrow have the same meaning as in Fig. 2(b).

α -SiO₂ films prepared by e -beam evaporation and wet thermal oxidation.¹⁹ Even more remarkable is that the Q_{film}^{-1} of the annealed film is a factor of 4 smaller than that of the as-sputtered film, thus being one order of magnitude below the lower limit of the “glassy range.” In contrast to the e -beam films, no relaxation peak can be resolved above 100 K in either the as-sputtered or annealed films.

The internal friction of a paddle with a 330 nm layer amorphized by ion-implantation is shown in Fig. 5(a). In addition to the temperature-independent internal friction below 10 K which is more than four times above the background of a bare paddle (solid line), a narrow relaxation peak occurs at 48 K. This peak has previously been identified as occurring in the heavily damaged crystalline region beneath the amorphous layer, and is believed to be caused by electronic relaxation of divacancy defects.⁴⁰ It will be ignored in the following discussion since it is not connected with the amorphous layer of interest. Rapid thermal annealing (RTA) at 850 °C for 30 s is known to lead to epitaxial regrowth of c -Si from the substrate.⁵¹ This RTA is performed on a companion as-implanted paddle, and its internal friction indeed fully recovers as shown in Fig. 5(a). Slow thermal annealing at 300 °C of another companion as-implanted paddle for 1 h leads to a complete disappearance of the relaxation peak as expected for the annealing behavior of divacancies,⁵³ while the temperature-independent internal friction develops some structure: the rise observed below 2 K is caused by some unidentified contamination resulting from the ion-implantation, although it affects the internal friction only after a slow anneal.⁵⁴ In addition to this and a small peak at 5 K, which we believe to originate from metastable states in the heavily damaged crystalline region beneath the amorphous layer as well, the plateau appears to be slightly reduced after annealing (by about a factor of 2). This can be viewed more clearly in Fig. 5(b) where Q_{film}^{-1} is shown. Annealing at 300 °C for 1 h will not induce epitaxial recrystallization.⁵¹ The internal friction plateau of the as-implanted α -Si is even smaller than that of the as-sputtered film by a factor of 1.7, demonstrating once again the importance of how the films were prepared.

From e -beam evaporation to amorphization by ion implantation, Q_0^{-1} is reduced by a factor of 4. Including the annealed, yet still fully amorphous films in this comparison, a decrease by a factor of 8 in Q_0^{-1} is obtained from the as- e -beam-evaporated to the sputtered-and-annealed α -Si films. This is a much larger variation than that commonly observed in other amorphous solids prepared by different techniques. For example, in heavily neutron-irradiated bulk α -SiO₂, low-temperature thermal conductivity and specific-heat measurements have indicated a decrease of Q_0^{-1} by a factor of 2 relative to that of well annealed, unirradiated α -SiO₂.⁵⁵ Compaction of bulk α -SiO₂ by 10% leads to a similar reduction of Q_0^{-1} as measured by low-temperature specific heat⁵⁶ and internal friction.⁵⁷ Effects of annealing were previously observed in some amorphous metal alloys. So far, the largest change was found in superconducting amorphous CuZr,⁵⁸ where a decrease of the internal friction by a factor of 3.5 was observed as well as an increase of the thermal conductivity by a factor of 2.5.

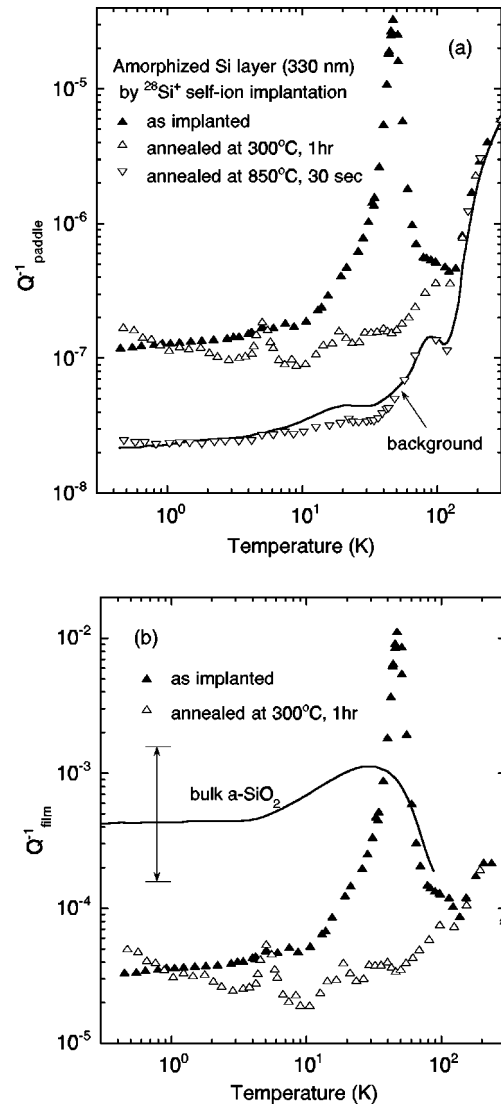


FIG. 5. (a) The internal friction of double-paddle oscillators carrying an amorphous layer prepared by $^{28}\text{Si}^+$ self-ion implantation: as implanted and annealed at 300 °C for 1 h. Also shown is the internal friction of a double-paddle oscillator carrying an identical implanted amorphous layer after a rapid-thermal anneal at 850 °C for 30 s so that the amorphous layer has undergone epitaxial recrystallization to the original crystalline structure. The background internal friction of a bare paddle oscillator is shown as a solid line for comparison. (b) The resulting internal friction of the same self-ion implanted amorphous layer, assuming that all the additional internal friction is within its 330 nm thick amorphous layer. However, the divacancies are actually confined to the damaged crystalline region about 70 nm thick underneath the amorphous layer (Ref. 40). Thus, the internal friction axis (Q_{film}^{-1}) is valid only for the amorphous layer. The solid line and double-arrow have the same meaning as in Fig. 2(b).

B. Internal friction of HWCVD α -Si:H films

We have reported previously that the low-temperature internal friction of HWCVD α -Si:H with about 1 at. % H is nearly three orders of magnitude smaller than that of any other known amorphous solid.²⁰ This is the first amorphous solid which does not have any significant low-energy excitations, in clear contrast to the universality established to date. This finding shows that the amorphous structure per se does

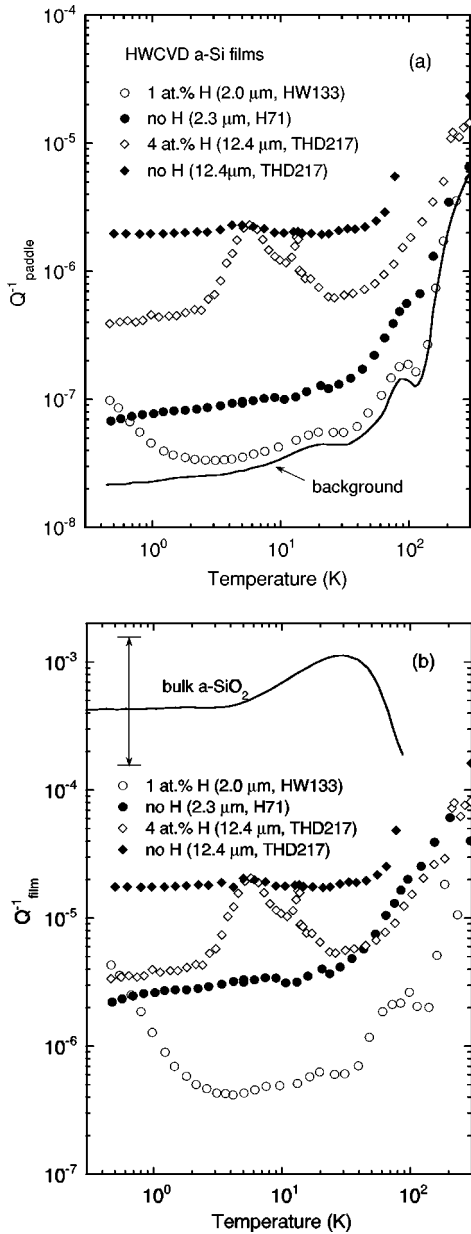


FIG. 6. (a) The internal friction of double-paddle oscillators with hot-wire chemical-vapor-deposited $a\text{-Si:H}$ films: sample HW133 is as-deposited with 1 at. % H. Sample H71, prepared under the same condition as sample HW133, is annealed in vacuum at 500°C for 24 h so that it does not contain any hydrogen in the film. Sample THD217 is as-deposited as well as annealed at 500°C for 24 h. The background internal friction of a bare paddle oscillator is shown as solid line. (b) The resulting internal friction of the same $a\text{-Si:H}$ films. The solid line and double arrow have the same meaning as in Fig. 2(b).

not lead to the glassy excitations. It also provides the opportunity to study the microscopic origin of the tunneling states by varying them in a controlled way. The internal friction of one of these samples (HW133, $2.0\ \mu\text{m}$ thick)²⁰ is shown in Fig. 6(a) as Q_{paddle}^{-1} vs T , with the solid line that of a bare paddle, and in Fig. 6(b) as Q_{film}^{-1} vs T where the solid line and double arrow are the internal friction of bulk $a\text{-SiO}_2$ and the “glassy range,” respectively, for comparison. The steep increase of Q^{-1} with decreasing temperature below 2 K in the film with 1 at. % H is caused by a contamination of the

silicon oscillator similar to that mentioned above after a slow anneal of an ion-implanted paddle oscillator, although the contaminants may be different.⁵⁴ As was shown previously,²⁰ increasing the H content above 1 at. % not only increases the internal friction over the entire temperature range, but also causes some structure as well. This is also illustrated in Figs. 6(a) and 6(b) with a $12.4\ \mu\text{m}$ thick film (THD217) which contains 4 at. % H. The double-peak structure between 3 and 15 K is attributed to the existence of molecular hydrogen and is the subject of a separate investigation.⁵⁹ The main point is that as the hydrogen concentration increases from 1 to 4 at. %, Q^{-1} increases by about one order of magnitude. This clearly demonstrates that while H is needed to eliminate the low-energy excitations of $a\text{-Si}$ films, excess H is detrimental to the elastic quality. This dependence on hydrogen is also in agreement with earlier surface acoustic-wave measurements, where a systematic increase of $\bar{P}\gamma^2$ with hydrogen content was observed in the relative variation of sound velocity in PECVD $a\text{-Si:H}$ films for H content larger than 14 at. %.¹⁷

In order to explore the role played by hydrogen in these HWCVD $a\text{-Si:H}$ films, we annealed both sample THD217 and a companion sample to HW133, labeled H71 ($2.3\ \mu\text{m}$ thick), at 500°C for 24 h. It is known that all the hydrogen will be driven out of the films by this annealing process, without leading to crystallization.⁵⁰ Figures 6(a) and (b) show that the internal friction increases, in contrast to the decrease resulting from annealing H-free $a\text{-Si}$ films presented in the previous subsection. Most remarkably, although both films (THD217 and H71) have experienced the same heat treatment and have the same zero-hydrogen content at the end of the process, their internal friction plateaus are different by a factor of 6. This observation indicates that the low-energy excitations in these amorphous films strongly depend on the original states formed during deposition, i.e., on the way that hydrogen is incorporated rather than the annealing process involved to remove hydrogen, reflecting the crucial role played by hydrogen in reducing the low-energy excitations in $a\text{-Si:H}$ films. The Q_0^{-1} of sample THD217 after driving off the hydrogen reaches a value close to that of the sputtered-and-annealed $a\text{-Si}$ (see Fig. 4), the lowest among the H-free $a\text{-Si}$ films.

C. Internal friction of $a\text{-Ge}$ films

Figure 7 shows the internal friction of $e\text{-beam}$ and sputtered $a\text{-Ge}$ films, both about $500\ \text{nm}$ thick. In contrast to $a\text{-Si}$ films where a difference of more than a factor of 2 in Q_0^{-1} between the $e\text{-beam}$ and the sputtered films is observed, there is almost no difference in these two as-deposited $a\text{-Ge}$ films. The internal friction plateaus of the two are smaller than that of $e\text{-beam}$ $a\text{-Si}$, but are almost the same as sputtered $a\text{-Si}$. Annealing at 350°C reduces Q_0^{-1} of the amorphous film by a factor of 3. So we conclude that similar to $a\text{-Si}$ films, $a\text{-Ge}$ films have the same low-energy excitations as all amorphous solids, but the internal friction plateau clearly falls below the universal values as indicated by the double arrow of the “glassy range” in Fig. 7. We tentatively attribute the similarity between $a\text{-Si}$ and $a\text{-Ge}$ films to their tetrahedrally coordinated bonding.

Similar to $e\text{-beam}$ $a\text{-Si}$ films, the internal friction of $e\text{-beam}$ $a\text{-Ge}$ films shows a relaxation peak at about 150 K in both as-evaporated and annealed form. A similar, but much

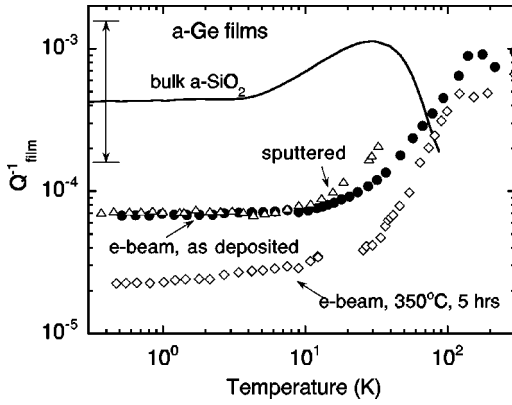


FIG. 7. The internal friction of *a*-Ge films: as *e*-beam evaporated, and after annealing at 350 °C for 5 h, and as sputtered. The solid line and double arrow have the same meaning as in Fig. 2(b).

sharper, peak was reported by Bhatia *et al.*¹⁴ in acoustic absorption of sputtered *a*-Ge films at 135 K using surface acoustic waves at 300 MHz, which they attributed to the motion of twofold-coordinated germanium atoms. If the broad peak observed in our internal friction measurement had the same origin, i.e., the same activation energy, it would appear below 135 K instead of at 150 K because of the smaller resonant frequency used here. This is in contrast to the case of *e*-beam *a*-Si films where a good agreement with the result of the surface acoustic waves was obtained (see subsection A). More accurate measurements at different frequencies are needed to elucidate this peculiar higher temperature feature. We believe that the study of the higher temperature feature is also interesting because the structural origin of thermally activated processes is relatively easy to locate and may well be closely related to that of the tunneling process occurring at low temperatures.⁶⁰

D. Relative variation of sound velocity of *a*-Si and *a*-Ge films

Characteristic differences between amorphous and crystalline solids also occur in the temperature variation of the sound velocity (see Sec. II). Below 1 K, the resonant scattering of sound waves by the tunneling states in amorphous solids leads to the logarithmic temperature variation of the sound velocity given by Eq. (2). This relation, which has frequently been used to extract the quantity *C* in ultrasonic measurements in the 10⁵ Hz range and above, is, however, not accessible for the frequencies used in the present study, because this logarithmic temperature dependence occurs at temperatures smaller than those available in our cryostat. In the temperature range above a few K and up to tens of K, it was found by Bellessa⁶¹ that, in a variety of amorphous solids, the sound velocity varies linearly with temperature as expressed by

$$\Delta v/v_0 = -\beta(T - T_0). \quad (8)$$

By compiling data on the linear variation of the sound velocity described by Eq. (8) and the Q_0^{-1} , White and Pohl⁶² recently summarized an empirical relation between the slope of the linear variation of sound velocity, β , and the internal friction plateau, Q_0^{-1} , which is given by

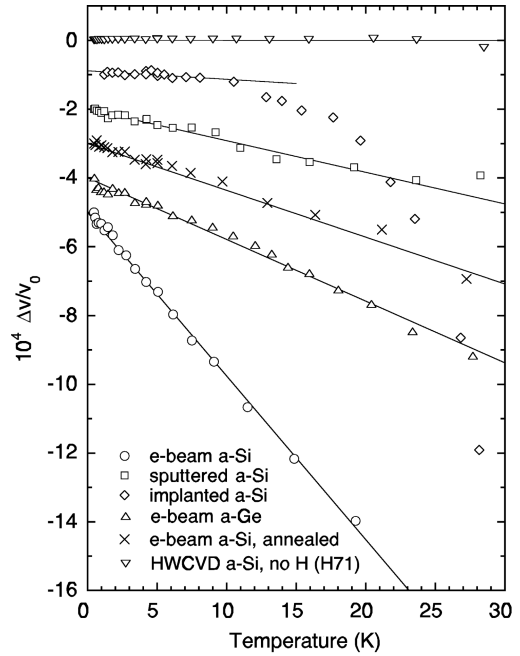


FIG. 8. The temperature variation of the sound velocity of selected *a*-Si(:H) and *a*-Ge films whose internal friction results have been presented in Figs. 2–7. The straight lines are linear fits from which the slopes of the linear temperature variation [see Eq. (8)] are determined.

$$\beta = 0.5 \cdot Q_0^{-1} (\text{K}^{-1}). \quad (9)$$

This relationship was found to hold not only for all amorphous solids studied, but also for disordered crystals. We have shown above that we are able to vary Q_0^{-1} for amorphous solids over three orders of magnitude by including *a*-Si and *a*-Ge films, and in particular *a*-Si:H films. These data can serve as an additional test of this intriguing but so far unexplained relation [Eq. (9)] over an extended range of Q_0^{-1} . The temperature dependence of $\Delta v/v_0$ of selected *a*-Si(:H) and *a*-Ge films are plotted in Fig. 8 calculated according to Eq. (7). Each curve is shifted by one unit on the vertical axis for clarity. Just as in all other amorphous solids,⁶² the linear temperature dependence is obvious. For the as-implanted *a*-Si layer the rapid dropoff of $\Delta v/v_0$ above 10 K is due to the influence of the divacancy peak in internal friction at 48 K occurring in the damaged crystalline region beneath the amorphous layer as mentioned above [see Figs. 5(a) and 5(b)]. In this case, we determine the slope only from data points below 10 K. The solid lines are linear fits from which the slopes β are obtained. The relation between β and Q_0^{-1} is shown in Fig. 9 for all samples investigated in this work except for HW133; for the paddle oscillator carrying this film the relative variation of its resonant frequency was too close to that of a bare paddle to permit a meaningful determination of $\Delta v/v_0$. Even for the other HWCVD films large error bars have to be included in determining β , which are shown in Fig. 9. The solid line in this figure expresses the relation given by Eq. (9). So we conclude that this relation is still valid when tetrahedrally bonded amorphous solids are included, certainly within the experimental accuracy encountered in the previous work.⁶² In spite of the experimental uncertainty, we may conclude that a close relation exists be-

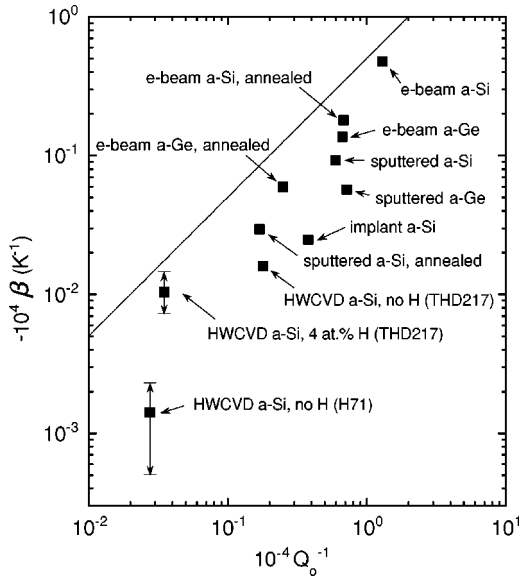


FIG. 9. A comparison of the slope of the linear temperature variation of sound velocity β [see Eq. (8)] with the internal friction plateau Q_0^{-1} for all the a -Si(:H) and a -Ge films presented in this work except for sample HW133, as explained in the text. The solid line indicates the empirical relation proposed in Ref. 62 [see also Eq. (9)]. The error bars indicate the uncertainty in determining β for those samples.

tween the quantity β and the magnitude of the plateau; as the latter vanishes, the former also disappears. This observation confirms that the Bellessa effect is related to the same defects which lead to the temperature-independent plateau of the internal friction.

VI. DISCUSSION

A. Comparison with earlier experiments

As a continuation of the short review presented in Sec. II, we will compare the results of our internal friction measurements with those of the earlier experiments. In Table I, the values of $\bar{P}\gamma^2$ and C determined in this work by the internal friction measurements using Eq. (4) are compared to those reviewed in Sec. II for similar deposition methods.

For specific-heat measurements, only upper limits of \bar{P} were given for e -beam a -Si (Ref. 11) and a -Ge films.^{8,9} However, using these values to calculate upper limits of $\bar{P}\gamma^2$ and C (by using the γ value mentioned in Sec. II) we obtain values which are close to those determined in this work. The comparison indicates that the residual anomalous specific heat observed in high magnetic fields, especially in the case of e -beam a -Si, may indeed have been caused by the low-energy excitations of the atomic tunneling states in the films.

The upper limits or the values of $\bar{P}\gamma^2$ and C of sputtered a -Si (Refs. 12,15) and a -Ge (Refs. 13,14) films determined by surface acoustic waves are also in reasonable agreement with those determined in this work. Note that the primary parameter determined by our internal friction measurements is $\bar{P}\gamma^2$ for the fact that the measured internal friction increase ($Q_{\text{paddle}}^{-1} - Q_{\text{bare}}^{-1}$) has to be divided by $G_{\text{film}} = \rho v^2$ to get C [see Eq. (5)], while C is the initial quantity obtained in measurements of the surface acoustic waves. We believe 10

and 60% reductions of ρ and v , respectively, have to be considered for the sputtered a -Ge films relative to those of bulk polycrystalline germanium (see Sec. IV). This makes ρv^2 three times smaller than that used in Ref. 13, which has to be taken into account in comparison. The important difference is that in this work we find that annealing of as-deposited a -Si and a -Ge films at 350 °C for 5 h reduces the internal friction plateau by a factor of 2–4, which is not observed in Ref. 13. For sputtered a -Si films measured by Tokumoto *et al.*,¹⁵ almost the same values of ρ and v were used as in the evaluation of this work. However, the values of $\bar{P}\gamma^2$ and C determined by Tokumoto *et al.* are considerably larger than those determined in this work. This is probably caused by the less sensitive measurements in the relative variation of frequency, resulting from the smaller film thicknesses than those used by Duquesne and Bellessa.¹³ We conclude that while the surface acoustic-wave technique may have just enough sensitivity to detect the low-energy excitations in the films, it may not be sensitive enough to distinguish the variations resulting from the different deposition methods and from heat treatment, which are identified in our present systematic study for the first time through low-temperature internal friction measurements. However, we suggest that a systematic study of the logarithmic temperature variation of sound velocity is still needed to show the dependence of the low-energy excitations on the modes of preparation and annealing, which is not covered in the present study.

Another interesting point is that among the studies using the surface acoustic wave technique, only Duquesne and Bellessa¹³ gave a consistent description of the relative variation of sound velocity and acoustic attenuation using the TLS model. In all the other studies,^{12,14,15} an attenuation shoulder at about 2 K was observed, which is similar to that of the sputtered a -Ge films found by Duquesne and Bellessa.¹³ However, none of these authors attributed its existence to the intrinsic tunneling states. Rather they suggested the cause to be oxygen impurities. Using the conversion factor introduced by Duquesne and Bellessa¹³ from transverse to surface waves, we find that the magnitude of these attenuation shoulders can yield values of $\bar{P}\gamma^2$ and C within a factor of 3 to those determined in this work, as summarized in Table I as well. Conceivably, it was the insufficient sensitivity that led to the conclusions reached in the earlier studies.

B. Low-energy excitations in a -Si and a -Ge films

Internal friction provides a sensitive probe of the relaxational processes of defect states in solids. Dissipation of energy occurs when $\omega\tau = 1$ is satisfied, where τ is the relaxation time of the defect states under the strain of sound waves with an angular frequency ω . In amorphous solids, the resonant contribution to Q^{-1} is negligible at the low frequencies used in our measurements. Tunneling states with a constant spectral density of states \bar{P} contribute a plateau in internal friction. However, there are other processes which may cause energy dissipation at low temperatures, thus interfering with the observation of the intrinsic structure-induced atomic tunneling states in internal friction measurements. We will discuss such possible influences here.

Although undoped a -Si and a -Ge films are electrically insulating at low temperatures, an electronic contribution to

Q^{-1} may still be possible due to the phonon-assisted hopping between localized electronic states. However, we believe that this is quite unlikely for the reason that even in pure, crystalline metal films the electronic contribution to the damping is negligibly small due to its short mean free path.³¹ Moreover, the electronic density of states near the Fermi level in *a*-Si and *a*-Ge films as estimated from the $T^{-1/4}$ law for the hopping conductivity⁶³ is about four orders of magnitude smaller than that in pure metal films.

It is well known that PVD *a*-Si and *a*-Ge films contain unpaired localized electrons up to a density of $N \approx 10^{19}$ to 10^{20} cm⁻³ mostly on sites of dangling bonds, as evidenced by electron-spin resonance¹⁶ and magnetic susceptibility⁶⁴ measurements. Magnetic moments of isolated unpaired electrons in *a*-Si and *a*-Ge films will experience dipolar interactions and hyperfine interactions between magnetic moments of the electrons and the nuclei.⁶⁵ Also, clustered electron spins have been found to have exchange-coupled interactions.^{16,8} According to Thomas *et al.*,¹⁶ annealing at 350 °C for 5 h reduces the spin density in *e*-beam *a*-Si by a factor of 2, which coincides with the reduction of Q_0^{-1} after the same annealing process observed in this work. The question then arises whether the internal friction plateau observed in our *a*-Si and *a*-Ge films may originate from magnetic excitations. So far, no direct evidence has been published as to whether these magnetic excitations affect the elastic and/or acoustic properties. We have recently measured the internal friction of *e*-beam *a*-Si films under high magnetic fields and found the value of Q_0^{-1} to be independent of the applied field up to 6 T, thus excluding magnetic excitations as a possible origin. The results will be published separately.⁶⁶

Incorporation of oxygen is known to cause atomic tunneling states inside the *a*-Si and *a*-Ge matrix^{12,14} which are not intrinsic to *a*-Si and *a*-Ge. Our samples were prepared with great care to minimize the oxygen content. Using RBS, both evaporated and sputtered samples were found to have oxygen within the detection limit (<1 at. %). For the *a*-Si layer produced by self-ion implantation, the oxygen content should be even less, within the limit of our superpure float-zone silicon wafer (<20 ppm). So oxygen should not be a problem in our internal friction measurements. However, we cannot exclude the influence of possible oxygen contamination as a cause for some of the contradictory early reports as reviewed in Sec. II.

Besides oxygen, some other impurities may enter into the *a*-Si and *a*-Ge films or the crystalline silicon substrates. They may form additional defect states. The contamination peak below 1 K that occurred during thermal annealing of paddle oscillators after ion-implantation or during hot-wire chemical-vapor deposition is an example, see Figs. 5 and 6. These defect states, presumably originating in the crystalline silicon substrates,⁵⁴ show temperature dependence in internal friction distinct from that of the tunneling states. These additional contributions can be easily separated.

We conclude that the low-energy excitations observed as a temperature-independent plateau in internal friction are indeed caused by the structurally induced tunneling states, common to all other amorphous solids.

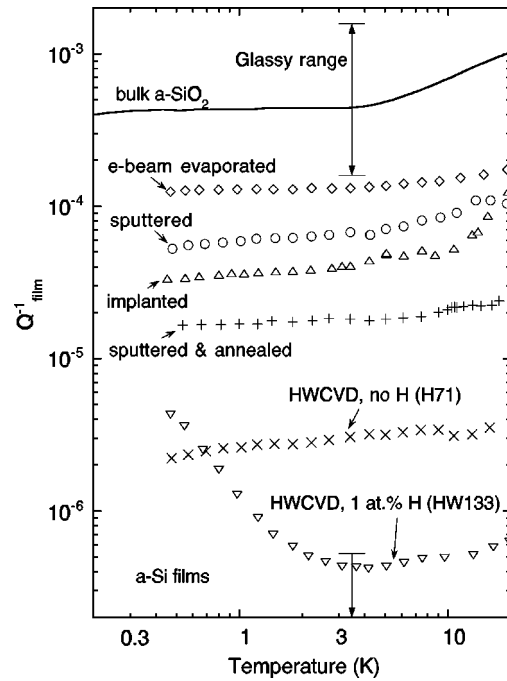


FIG. 10. The internal friction of selected *a*-Si and *a*-Si:H films presented in this work. The solid line and double arrow have the same meaning as in Fig. 2(b). The single arrow indicates the uncertainty in determining Q_{film}^{-1} for that sample.

C. What became of the “universality”?

To emphasize the dramatic dependence of the internal friction plateau on the modes of preparation, thermal annealing, and hydrogenation, we have collected in Fig. 10 some representative internal friction results of *a*-Si and *a*-Si:H films for comparison. Between films prepared by *e*-beam evaporation and films prepared by HWCVD with 1 at. % H, Q_0^{-1} is seen to vary by more than two orders of magnitude. The error bar for the HWCVD *a*-Si:H with 1 at. % H indicates the experimental uncertainty in the determination of the Q_0^{-1} in that case since there is essentially no damping excess over the background except for the contamination peak which occurs below 1 K mentioned in Sec. V. If we compare these data with the internal friction of bulk *a*-SiO₂ and the “glassy range” also shown in Fig. 10, it is quite obvious that the universality of the low-energy tunneling states, which had been established without exceptions for the past 27 years, does not hold anymore. Since all of these silicon films are clearly structurally amorphous, it follows that the amorphous structure alone is insufficient to cause the glassy low-energy states. The possible cause for the variability and nearly complete disappearance of the low-energy excitations will be discussed below.

An amorphous solid having a *perfect* tetrahedrally bonded continuous random network is rigid and may be expected³ to have none of the atomic tunneling states which had been postulated in the TLS model, because the appearance of tunneling states requires more than one equilibrium position of the tunneling entities. This idea has been elaborated with the constraint-counting model,^{67,68} which is believed to govern the elastic and vibrational properties of amorphous solids. The predicted floppy-rigid transition has been found in good agreement with experimental investigations.⁶⁹ Its impact on

the low-energy tunneling states has also been evidenced qualitatively in low-temperature specific-heat measurements.⁷⁰ Conceivably, the low-temperature internal friction observed in the present work may be a direct consequence of the unique tetrahedrally bonded amorphous structure in *a*-Si and *a*-Ge films.

For *a*-Si(:H) and *a*-Ge films prepared under various non-equilibrium conditions, local floppy modes might arise from locally defective, effectively underconstrained, regions due to the internal or growth strains in an otherwise overconstrained network. Molecular-dynamics simulations^{71,72} show that the existence of twofold- and threefold-coordinated sites leads to vibration localization which may be closely related to the atomic tunneling states observed in amorphous solids. Amorphous Si and Ge films deposited near room temperature are granular, even porous. When annealed at elevated temperatures, but well below the crystallization temperature, they undergo significant structural relaxation toward a more continuous random structure in which the underconstrained regions are reduced.⁷³ In *a*-Si films prepared by ion implantation, enthalpy release during annealing below the crystallization temperature has been studied.⁷⁴ This release is accompanied by a reduction of bond-angle distribution,⁷⁵ thus demonstrating a significant structural relaxation with increasing short-range order. Evidence of a reduction of the bond angle distribution and of a subsequent densification and homogenization after annealing has also been found for *a*-Si (Refs. 76,77) and *a*-Ge (Refs. 73,78) films prepared either by *e*-beam evaporation or by sputtering in structural and calorimetric studies. The observed structural relaxation upon thermal annealing may be closely related to the change in the density of the low-energy tunneling states as measured by the internal friction.

Although annealed *a*-Si films have lower free energy than as-deposited ones,⁷⁶ there may be a limit below which the low-energy excitations cannot be decreased by thermal annealing alone. Recent study of coherent transmission electron microscopy⁷³ shows that annealing *e*-beam *a*-Ge film increases short-range order at the expense of medium-range order. This may be related to the difficulty encountered during conventional deposition and annealing to nucleate a continuous random network. In addition, building a tetrahedrally bonded continuous random network may inevitably cause clusters of dangling bonds to occur as a result of accumulated local strains. Incorporation of hydrogen may therefore be a necessary step not only to passivate the dangling bonds but also to relieve the strain in the amorphous matrix^{72,79} in order to extend the medium-range order, which is indeed observed in HWCVD *a*-Si:H films by x-ray diffraction.⁴⁷ The structure of the resulting material may be closer to a *perfect* continuous random network than any other forms of *a*-Si studied so far.

Since H-terminated Si lacks the full tetrahedral connectivity of the network, additional local floppy modes may result as the H content exceeds the level which is needed to passivate the dangling bonds and to relieve the strain. As a result, the density of the tunneling states increases with excess hydrogen.

Removal of hydrogen by an anneal at 500 °C may cause the already near-perfect continuous random network energetically unfavorable. The film may eventually recover the

highly strained regions which drive it into a less perfect structure, similar to the well-relaxed state in H-free *a*-Si films. An interesting observation is that the low-energy excitations in these hydrogen-free HWCVD *a*-Si films depend sensitively on the initial deposition conditions which had led to different hydrogen content in the as-deposited films. This reveals the profound role played by hydrogen during deposition in producing an equilibrium microscopic structure that partially remains even after the hydrogen has been removed.

It is worth noting that the experimentally determined floppy-rigid transition threshold has frequently been found to be higher than the predicted value of the mean-field theory.⁸⁰ The imperfection of the structure due to the existence of locally unconnected or weakly connected bonds may contribute to the discrepancy. Therefore, we emphasize that local fluctuations should be included in the constraint-counting model, which sometimes may dominate the lattice vibrations of overall overconstrained continuous random networks, as in the case of *a*-Si and *a*-Ge films.

Another parameter which may be crucial in determining the existence of tunneling states is the random strain in amorphous solids. Its role in generating the low-temperature glassy behavior in the mixed crystal (KCl)_{0.5}(KBr)_{0.5} + 0.9% CN has been demonstrated by Watson.⁸¹ It has been found recently that hydrogenation with 1–2 at. % H of *a*-Si by HWCVD effectively relieves the internal compressive strain.⁸² We suggest that while amorphicity is not a sufficient condition for tunneling states, the existence of random strain may be a necessary condition.

It has been proposed recently by Kühn and Horstmann⁸³ that amorphous phases without low-energy tunneling states may exist, although the criteria given have not been applicable to real amorphous systems. We hope the results presented here will inspire both experimental and theoretical studies in identifying the nature of the low-energy excitations of amorphous solids.

VII. CONCLUSION

Unlike all other amorphous solids studied so far, the low-energy excitations in *a*-Si and *a*-Ge films show a wide variation, deviating from the universality established for all other amorphous solids without exceptions for the past 27 years. Their magnitude, as determined by the temperature-independent internal friction plateau below 10 K, is below the lower limit of the “glassy range” (1.5×10^{-3} – 1.5×10^{-4}), in which all other amorphous solids have been found to lie, and furthermore diminishes by more than two orders of magnitude when HWCVD *a*-Si:H films are included. Film preparation methods, heat treatment, and incorporation of hydrogen are found to be the parameters leading to the dramatic changes of the tunneling states. However, the connection of film preparation and thermal treatment with the tunneling states is complicated. While annealing decreases the internal friction of H-free *a*-Si and *a*-Ge films, removal of hydrogen by annealing of HWCVD *a*-Si:H films increases the internal friction, demonstrating the profound role played by hydrogen in reducing the tunneling states.

We have reviewed the earlier experimental investigations in both H-free and hydrogenated *a*-Si and *a*-Ge films, and compare those with our results of the internal friction mea-

surements. We conclude that the previous reports of contradictory observations are mainly caused by inadequate sensitivity of the techniques applied together with the possible influence of film preparation conditions, e.g., incorporation of impurities. In addition, earlier investigations are far from systematic so that comparison between results of differently prepared samples may add further complication to the limited sensitivity.

We suggest that the peculiar properties of the low-energy excitations in these thin amorphous films may be related to their unique tetrahedrally bonded structure which is globally overconstrained. The atomic motion, which is a prerequisite for tunneling states at low temperatures, may originate from the locally underconstrained regions, and may therefore be sensitively dependent on the perfection of the covalent continuous random network. It may be that the tunneling states are caused by loosely bonded individual atoms or clusters of atoms as suggested by Phillips.³ Incorporation of small amounts of hydrogen is found to be an effective way to annihilate the low-energy excitations. However, the exact role played by hydrogen, especially its structural relation to the atomic tunneling states in addition to its passivating the dangling bonds and relieving the strains, is still not understood. It is encouraging that the same thin-film material in which we find the disappearance of the low-energy tunneling states also exhibits better device quality as a semiconductor.⁸⁴ There is a striking parallel between the minimum in the Q_0^{-1}

with the H content and the minimum in both light-induced⁸⁵ and thermally induced⁸⁶ metastability, indicating a possible relation between the low-energy excitations discussed here and the electronic and optical properties of these semiconductors.

ACKNOWLEDGMENTS

We are grateful for Dr. R. S. Crandall for many stimulating discussions. We acknowledge Dr. E. Iwanizcko, A. H. Mahan, K. M. Jones, T. E. Furtak, and D. L. Williamson for preparations and characterizations of the HWCVD *a*-Si:H thin films used in this work. We thank Dr. P. Wagner from Wacker Siltronic in Burghausen, Germany, for supplying us with the ultrapure silicon wafers, from which the double-paddle oscillators were made. We also thank Dr. G. Wilk from Texas Instruments Inc. at Dallas, Texas for growing the MBE silicon film, and Dr. P. Revesz at Cornell Ion Beam Laboratory for the RBS/channeling measurements. This work was supported by the Semiconductor Research Corporation under Grant No. 95/Sc/069, the National Science Foundation under Grant No. DMR-9701972, the NREL FIRST Program, and the DOE under Contract No. DE-ACO2-83CH10093. Additional support was received from the National Nanofabrication Facility at Cornell University, NSF Grant No. ECS-9319005.

*Electronic address: pohl@msc.cornell.edu

¹R. C. Zeller and R. O. Pohl, Phys. Rev. B **4**, 2029 (1971).

²P. W. Anderson, B. I. Halperin, and C. M. Varma, Philos. Mag. **25**, 1 (1972).

³W. A. Phillips, J. Low Temp. Phys. **7**, 351 (1972).

⁴*Amorphous Solids: Low Temperature Properties*, edited by W. A. Phillips (Springer-Verlag, Berlin, 1981).

⁵H. v. Löhneysen and F. Steglich, Phys. Rev. Lett. **39** 1420 (1977).

⁶J. E. Graebner and L. C. Allen, Phys. Rev. Lett. **51**, 1566 (1983); Phys. Rev. B **29**, 5626 (1984).

⁷C. N. King, W. A. Phillips, and J. P. deNeufville, Phys. Rev. Lett. **32**, 538 (1974).

⁸H. v. Löhneysen and H. J. Schink, Phys. Rev. Lett. **48**, 1121 (1982).

⁹R. van den Berg and H. v. Löhneysen, Phys. Rev. Lett. **55**, 2463 (1985).

¹⁰M. Mertig, G. Pompe, and E. Hegenbarth, Solid State Commun. **49**, 369 (1984).

¹¹R. van den Berg, H. v. Löhneysen, and H. J. Schink, J. Non-Cryst. Solids **77&78**, 1339 (1985).

¹²M. v. Haumer, U. Strom, and S. Hunklinger, Phys. Rev. Lett. **44**, 84 (1980).

¹³J. Y. Duquesne and G. Bellessa, J. Phys. C **16**, L65 (1983); Philos. Mag. B **52**, 821 (1985).

¹⁴K. L. Bhatia and S. Hunklinger, Solid State Commun. **47**, 489 (1983).

¹⁵H. Tokumoto, K. Kajimura, S. Yamasaki, and K. Tanaka, *Proceedings of the 17th International Conference on Low Temperature Physics*, edited by U. Eckern, A. Schmid, W. Weber, and H. Wühl (North-Holland, Amsterdam, 1984), p. 381.

¹⁶P. A. Thomas, M. H. Brodsky, D. Kaplan, and D. Lepine, Phys. Rev. B **18**, 3059 (1978).

¹⁷H. Tokumoto, K. Kajimura, S. Yamasaki, and K. Tanaka, *Proceedings of the 17th International Conference on Physics of Semiconductors*, edited by J. D. Chadi and W. A. Harrison (Springer-Verlag, New York, 1984), p. 829.

¹⁸B. E. White, Jr. and R. O. Pohl, in *Thin Films: Stresses and Mechanical Properties V*, edited by S. P. Baker *et al.*, MRS Symposia Proceedings No. 356 (Materials Research Society, Pittsburgh, 1995), p. 567.

¹⁹B. E. White, Jr. and R. O. Pohl, Phys. Rev. Lett. **75**, 4437 (1995).

²⁰X. Liu, B. E. White, Jr., R. O. Pohl, E. Iwanizcko, K. M. Jones, A. H. Mahan, B. N. Nelson, R. S. Crandall, and S. Veprek, Phys. Rev. Lett. **78**, 4418 (1997).

²¹K. A. Topp and D. G. Cahill, Z. Phys. B **101**, 235 (1996).

²²J. F. Berret and M. Meissner, Z. Phys. B **70**, 65 (1988).

²³U. Buchenau, M. Prager, W. A. Kamitakahara, H. R. Shanks, and N. Nücker, Europhys. Lett. **6**, 695 (1988).

²⁴P. A. Medwick, B. E. White, Jr., and R. O. Pohl, J. Alloys Compd. **270**, 1 (1998).

²⁵For energy decay or absorption, we have the numerical relation: $Q^{-1} = 0.23(v/\omega)\alpha$ where α is in dB/cm, v in cm/s, and ω in radian/s.

²⁶H. v. Löhneysen, H. Rüsing, and W. Sander, Z. Phys. B **60**, 323 (1985).

²⁷H. v. Löhneysen, J. Non-Cryst. Solids **59&60**, 1087 (1983).

²⁸J. E. Graebner, B. Golding, L. C. Allen, J. C. Knights, and D. K. Biegelsen, Phys. Rev. B **29**, 3744 (1984).

²⁹K. L. Bhatia, M. v. Haumer, and S. Hunklinger, Solid State Commun. **37**, 943 (1981).

³⁰K. L. Bhatia, M. v. Haumer, and S. Hunklinger, Z. Phys. B **44**, 155 (1981).

³¹X. Liu, E. J. Whang, B. E. White, Jr., and R. O. Pohl (unpublished).

- ³²G. Simmons and H. Wang, *Single Crystal Elastic Constants and Calculated Aggregate Properties: A Handbook* (The M.I.T. Press, Cambridge, Massachusetts, 1971).
- ³³B. E. White, Jr., J. Hessinger, and R. O. Pohl, *J. Low Temp. Phys.* **111**, 233 (1998).
- ³⁴H. J. McSkimin, *J. Appl. Phys.* **24**, 988 (1953).
- ³⁵I. R. Cox-Smith, H. C. Liang, and R. O. Dillon, *J. Vac. Sci. Technol. A* **3**, 674 (1985).
- ³⁶D. L. Williamson, S. Roorda, M. Chicoine, R. Tabti, P. A. Stolk, S. Acco, and F. W. Saris, *Appl. Phys. Lett.* **67**, 226 (1995).
- ³⁷M. Ohring, *The Material Science of Thin Films* (Academic, New York, 1992), pp. 79.
- ³⁸R. Vacher, H. Sussner, and M. Schmidt, *Solid State Commun.* **34**, 279 (1980).
- ³⁹L. R. Testardi and J. J. Hauser, *Solid State Commun.* **21**, 1039 (1977).
- ⁴⁰X. Liu, R. O. Pohl, R. S. Crandall, and K. M. Jones, in *Defects and Diffusion in Silicon Processing*, edited by S. Coffa *et al.*, MRS Symposia Proceedings No. 469 (Materials Research Society, Pittsburgh, 1997), p. 419.
- ⁴¹S. I. Tan, B. S. Berry, and B. L. Crowder, *Appl. Phys. Lett.* **20**, 88 (1972).
- ⁴²R. A. Street, *Hydrogenated Amorphous Silicon* (Cambridge University Press, Cambridge, United Kingdom, 1991).
- ⁴³R. S. Crandall, Y. S. Tsuo, Y. Xu, A. H. Mahan, and D. L. Williamson, *Sol. Cells* **30**, 15 (1991).
- ⁴⁴A. H. Mahan, J. Carapella, B. P. Nelson, R. S. Crandall, and I. Balberg, *J. Appl. Phys.* **69**, 6728 (1991).
- ⁴⁵P. C. Taylor, in *Semiconductors and Semimetals, Vol. 21C*, edited by J. I. Pankove (Academic, New York, 1984), pp. 99.
- ⁴⁶Y. Wu, J. T. Stephen, D. X. Han, J. M. Rutland, R. S. Crandall, and A. H. Mahan, *Phys. Rev. Lett.* **77**, 2049 (1996).
- ⁴⁷A. H. Mahan, D. L. Williamson, and T. E. Furtak, in *Amorphous and Microcrystalline Silicon Technology—1997*, edited by M. Hack *et al.*, MRS Symposia Proceedings No. 467 (Materials Research Society, Pittsburgh, 1997), p. 657.
- ⁴⁸A. Uhlherr and S. R. Elliot, *Philos. Mag.* **B 71**, 611 (1995).
- ⁴⁹A. A. Langford, M. L. Fleet, B. P. Nelson, W. A. Lanford, and N. Maley, *Phys. Rev. B* **45**, 13 367 (1992).
- ⁵⁰Z. Remes, M. Vanecek, A. H. Mahan, and R. S. Crandall, *Phys. Rev. B* **56**, R12 710 (1997).
- ⁵¹G. L. Olson and J. A. Roth, *Mater. Sci. Rep.* **3**, 1 (1988).
- ⁵²J. E. van Cleve, Ph.D. thesis, Cornell University, 1991; Suprasil-W is a type of α -SiO₂ which contains less than 1.5 ppm hydroxyl.
- ⁵³H. J. Stein, F. L. Vook, and J. A. Borders, *Appl. Phys. Lett.* **14**, 328 (1969).
- ⁵⁴X. Liu, R. O. Pohl, S. Asher, and R. S. Crandall, *J. Non-Cryst. Solids* **227-230**, 407 (1998).
- ⁵⁵A. K. Raychaudhuri and R. O. Pohl, *Solid State Commun.* **37**, 103 (1980); **44**, 711 (1982).
- ⁵⁶X. Liu, H. v. Löhneysen, G. Weiss, and J. Arndt, *Z. Phys. B* **99**, 49 (1995).
- ⁵⁷G. Weiss, A. Daum, M. Sohn, and J. Arndt, *Physica B* **219&220**, 290 (1996).
- ⁵⁸P. Esquinazi and J. Luzuriaga, *Phys. Rev. B* **37**, 7819 (1988).
- ⁵⁹X. Liu, E. Iwaniczko, R. O. Pohl, and R. S. Crandall, in *Amorphous and Microcrystalline Silicon Technology—1998*, edited by S. Wagner *et al.*, MRS Symposia Proceedings No. 507 (Materials Research Society, Pittsburgh, to be published).
- ⁶⁰D. Tielburger, R. Merz, R. Ehrenfels, and S. Hunklinger, *Phys. Rev. B* **45**, 2750 (1992).
- ⁶¹G. Bellessa, *Phys. Rev. Lett.* **40**, 1456 (1978).
- ⁶²B. E. White, Jr. and R. O. Pohl, *Z. Phys. B* **100**, 401 (1996).
- ⁶³N. F. Mott and E. A. Davis, *Electronic Processes in Non-Crystalline Materials*, 2nd ed. (Clarendon, Cambridge, England, 1979).
- ⁶⁴S. J. Hudgens, *Phys. Rev. B* **14**, 1547 (1976).
- ⁶⁵B. Movaghar, L. Schweitzer, and H. Overhof, *Philos. Mag. B* **37**, 683 (1978).
- ⁶⁶T. H. Metcalf *et al.* (unpublished).
- ⁶⁷J. C. Phillips, *J. Non-Cryst. Solids* **34**, 153 (1979).
- ⁶⁸M. F. Thorpe, *J. Non-Cryst. Solids* **57**, 355 (1983).
- ⁶⁹X. Feng, W. J. Bresser, and P. Boolchand, *Phys. Rev. Lett.* **78**, 4422 (1997), and references therein.
- ⁷⁰O. Brand and H. v. Löhneysen, *Europhys. Lett.* **16**, 455 (1991); X. Liu and H. v. Löhneysen, *Phys. Rev. B* **48**, 13 486 (1993).
- ⁷¹R. Biswas, A. M. Bouchard, W. A. Kamitakahara, G. S. Grest, and C. M. Soukoulis, *Phys. Rev. Lett.* **60**, 2280 (1988).
- ⁷²P. A. Fedders and D. A. Drabold, *Phys. Rev. B* **53**, 3841 (1996).
- ⁷³J. M. Gibson and M. M. J. Treacy, *Phys. Rev. Lett.* **78**, 1074 (1997).
- ⁷⁴S. Roorda, W. C. Sinke, J. M. Poate, D. C. Jacobson, S. Dierker, B. S. Dennis, D. J. Eaglesham, F. Spaepen, and P. Fuoss, *Phys. Rev. B* **44**, 3702 (1991), and references therein.
- ⁷⁵J. Fortner and J. S. Lannin, *Phys. Rev. B* **37**, 10 154 (1988).
- ⁷⁶R. R. De Avillez, L. A. Clevenger, and C. V. Thompson, *J. Mater. Res.* **4**, 1057 (1989).
- ⁷⁷J. C. Fan and C. Anderson, *J. Appl. Phys.* **52**, 4003 (1981).
- ⁷⁸P. Viscor, *J. Non-Cryst. Solids* **101**, 170 (1988).
- ⁷⁹P. P. Paduschek, Ch. Hopfl, and H. Mitlehner, *Thin Solid Films* **110**, 291 (1983).
- ⁸⁰J. Y. Duquesne and G. Bellessa, *Europhys. Lett.* **9**, 453 (1989); K. Tanaka, *Phys. Rev. B* **39**, 1270 (1989).
- ⁸¹S. K. Watson, *Phys. Rev. Lett.* **75**, 1965 (1995).
- ⁸²D. Han, T. Gotoh, M. Nishio, T. Sakamoto, S. Nonomura, S. Nitta, Q. Wang, and E. Iwaniczko, in *Thin Films—Stresses and Mechanical Properties VII*, edited by R. C. Cammarata *et al.*, MRS Symposia Proceedings No. 505 (Materials Research Society, Pittsburgh, 1997).
- ⁸³R. Kühn and U. Horstmann, *Phys. Rev. Lett.* **78**, 4067 (1997).
- ⁸⁴R. S. Crandall, X. Liu, and E. Iwaniczko, *J. Non-Cryst. Solids* **227-230**, 23 (1998).
- ⁸⁵A. H. Mahan and M. Vanecek, in *Amorphous Silicon Materials and Solar Cells*, edited by B. L. Stafford (AIP, New York, 1991), p. 195.
- ⁸⁶M. Vanecek and A. H. Mahan, *J. Non-Cryst. Solids* **190**, 163 (1995).